European Journal of Histochemistry 2025; volume 69:4218

Tanshinone IIA attenuates hepatic stellate cell activation, oxidative stress, and liver fibrosis by inhibiting YAP signaling

Dan Wang,[1]* Qingquan Tan,[2]* Qing Zheng,[1] Yanling Ma,[3] Li Feng[1]

[1]Division of Liver Surgery, Department of General Surgery and Regeneration Medicine Research Center, West China Hospital of Sichuan University, Chengdu, Sichuan
[2]Division of Pancreatic Surgery, Department of General Surgery, West China Hospital of Sichuan University, Chengdu, Sichuan
[3]Department of Oncology Surgery, Second Hospital of Lanzhou University, Lanzhou, Gansu, China

*These authors contributed equally to this work.

ABSTRACT

Tanshinone IIA is derived from *Salvia miltiorrhiza* and has multiple therapeutic targets and functions. The exact therapeutic effects on liver fibrosis as well as the underlying hepatoprotective mechanisms are still lacking. A liver fibrosis model was established *via* ligation of the common bile duct ligation (BDL). The mice were intraperitoneally administered different concentrations of tanshinone IIA (4 mg/kg, 8 mg/kg) for 2 weeks. Liver function was assessed through hematoxylin and eosin and Sirus red staining. Serum levels of aspartate aminotransferase (AST), alanine aminotransferase (ALT), glutathione (GSH) and malondialdehyde (MDA) were quantified by enzyme-linked immunosorbent assay (ELISA), *via* microplate reader. The total iron content of the liver was quantified *via* Triple Quad-ICP-MS. TGFβ-induced hepatic stellate cells (HSCs), a cell model of liver fibrosis, were treated with tanshinone IIA at different concentrations (10 mM, 20 mM, 30 mM, 40 mM). The combination of tanshinone IIA with YAP agonists was applied in activated HSCs and animal models. Tanshinone IIA treatment relieved BDL-induced liver fibrosis; mitigated histological liver damage; lowered the serum ALT and AST levels; reduced macrophage infiltration and the MDA and iron contents; and increased the GSH and GPX4 levels by inhibiting YAP signaling. tanshinone IIA also suppressed the activation of HSCs and collagen production through blocking the YAP signaling pathway. The YAP agonist reversed the therapeutic effect of tanshinone IIA on activated HSCs and BDL-induced liver fibrosis. Tanshinone IIA inhibited HSC activation and oxidative stress and alleviated liver fibrosis by inhibiting the YAP signaling pathway.

Key words: Tanshinone IIA; oxidative stress; hepatic stellate cells; liver fibrosis; YAP.

Correspondence: Li Feng, Regeneration Medicine Research Center, West China Hospital, Sichuan University, Chengdu, Sichuan, 610041, China. E-mail: fengli@scu.edu.cn

Contributions: LF, conceptualization, manuscript review and editing; DW, QT, QZ, methodology, software; DW, QT, QZ, YM, investigation; DW, QT, manuscript original drafting. All authors have read and agreed to the published version of the manuscript.

Conflict of interest: the authors declare no conflict of interest and all authors confirm accuracy.

Ethical approval: the present study was approved by the Ethics Committee of the West China Hospital of Sichuan University (approval no. 20220629004).

Availability of data and materials: the data used to support the findings of this study are available from the corresponding author upon reasonable request.

Funding: this research did not receive any specific grant from funding agencies in the public, commercial, or not-for-profit sectors.

Introduction

Liver fibrosis is a chronic wound-healing response caused by hepatitis B virus infection, hepatitis C virus infection, alcohol-associated liver disease, and nonalcoholic fatty liver disease, characterized by excessive deposition of the extracellular matrix (ECM) and continuous damage to liver parenchyma regeneration, eventually leading to cirrhosis and liver cancer if left untreated.[1,2] Liver fibrosis is an important public health problem, leading to 1.16 million deaths worldwide.[3,4] Although many preclinical trials have made considerable progress, the clinical trial outcome is still unsatisfactory, especially given that there is no effective antifibrotic therapy.[5,6] Currently, the only available treatments include the elimination of chronic stress and liver transplantation.[7] Hence, exploration of drugs that shield or alleviate liver fibrosis to improve the quality of life of patients holds substantial promise.

Hepatic stellate cells (HSCs), pivotal non-parenchymal cells located in the Disse space, are believed to be a cellular source of ECM following the activation of HSCs into myofibroblasts (MFs).[8,9] Therefore, targeted inhibition of HSC activation is an effective strategy to prevent and treat liver fibrosis. The Hippo-YAP-TAZ pathway can coordinate cell state transitions. Dysregulated pathway activity occurs in various maladaptive regenerative pathologies, including cancer and liver fibrosis.[10] In liver fibrosis, YAP orchestrates the transdifferentiation of resting HSCs to MFs and is upregulated during liver injury and liver fibrosis, promoting the proliferation and activation of HSCs.[11,12] In addition, some studies have shown that induced consumption of YAP can alleviate liver damage and fibrosis.[10] Therefore, inhibiting HSC activation through hindering YAP seems to be a feasible approach. In chronic liver disease, the accumulation of iron exacerbates damage to liver cells through oxidative stress mechanisms, leading to the progression of fibrosis. Excess iron in the liver can cause the formation of free radicals, damage cell membranes and DNA, and lead to the apoptosis and necrosis of hepatocytes.[13] In addition, acute liver injury and liver fibrosis can be alleviated by inhibiting ferroptosis through the regulation of YAP.[14] Thus, the YAP protein is associated with the iron load associated with liver fibrosis. YAP can also regulate macrophage polarization and participate in tissue repair, fibrosis and tumor microenvironment regulation.[15] The polarization of macrophages can affect the process of liver fibrosis: the activation of M1 macrophages can aggravate liver inflammation and the development of fibrosis. M2 macrophages can inhibit the inflammatory response and slow the process of fibrosis.[15] *Salvia miltiorrhiza* is a traditional Chinese medicine first recorded in Shenlong Materia Medica;[16] it has a variety of pharmacological activities, such as anti-inflammatory, antioxidant, and antifibrotic effects, reduces pain and improves blood circulation.[17,18] Tanshinone IIA, which is extracted from the root of *S. miltiorrhiza*, has a variety of pharmacological activities and has been widely used in Eastern countries for decades for the treatment of inflammation, oxidative stress and organ fibrosis.[19] It has proven to be safe enough, with few side effects.[20] A preclinical meta-analysis revealed that tanshinone IIA may improve liver function and liver fibrosis in experimental animals by reducing inflammation, suppressing immune and antiapoptotic processes, and inhibiting HSC activation.[21] At present, the therapeutic effect of tanshinone IIA on liver fibrosis has been reported only sporadically and has not been clearly confirmed.[22] There are few relevant basic studies, which are not deep enough and involve only a CCl4-induced model.[23,24] Therefore, whether tanshinone IIA can improve liver fibrosis by regulating YAP-regulated HSC activation, iron loading, and macrophage polarization has attracted our interest. The bile duct ligation (BDL) model is also a classic model of liver fibrosis, representing a clinical cholestasis disease, and no studies have investigated the effects of tanshinone IIA in a BDL model. our team established a BDL model, defined the therapeutic effect of tanshinone IIA on liver fibrosis, and reported that tanshinone iia relieves liver fibrosis by inhibiting yap signaling.

Materials and Methods

Animals and experimental protocol

Male C57BL/6 mice (6-8 weeks of age, weighing 18-22 g) were obtained from the Beijing Weitonglihua Laboratory Animal Center (Beijing, China). The animals were kept in a constant-temperature environment and supplied with laboratory chow and water ad libitum. The animal experiments were divided into two parts: the first part aimed to verify the therapeutic effect of tanshinone IIA on liver fibrosis, and the second part aimed to verify the effect of YAP agonists on the therapeutic effect of tanshinone IIA. The 24 male mice were randomly divided into 4 groups: the sham group (Sham), the BDL group (BDL), the tanshinone IIA 4 mg/kg+BDL group (tanshinone IIA 4), and the tanshinone IIA 8 mg/kg+BDL group (tanshinone IIA 8). In the second part, 24 male mice were randomly divided into 4 groups: the sham group (Sham), the BDL group (Model), the tanshinone IIA 8 mg·kg-1+BDL group (tanshinone IIA 8), and the tanshinone IIA 8 mg/kg+BDL group (tanshinone IIA 8)+ XMU-MP-1 (YAP agonist) 1 mg/kg (tanshinone IIA 8+XMU). The mice were anesthetized with 40 mg/kg pentobarbital sodium, the pain reflex disappeared, the abdominal fur was shaved, the abdominal wall was disinfected, the common bile duct between the hilum and the duodenum was freed, and the mice were observed for 2 weeks. The sham-operated group underwent laparotomy but not ligation. Tanshinone IIA (MedChemExpress LLC, Monmouth Junction, NJ, USA) was injected intraperitoneally once a day after bile duct ligation. Tanshinone IIA was dissolved in a saline solution containing 0.5% CMC-Na and 0.1% Tween-80. The mice in the control and model groups were given the same amount of solvent (saline solution containing 0.5% CMC-Na and 0.1% Tween-80). In the second part, XMU-MP-1 (Selleck Chemicals, Houston, TX, USA) dissolved in a solvent (5% DMSO+40% PEG300+5% Tween 80+50% ddH_2O) was injected intraperitoneally once a day, and the time interval between the two drugs was 8 h. After 2 weeks, all the mice were euthanized with an overdose of pentobarbital sodium (200 mg/kg), and the livers were harvested. All procedures performed on mice were in compliance with the ARRIVE guidelines and in accordance with relevant guidelines and regulations. The research was approved by the Ethics Committee of the West China Hospital of Sichuan University (approval no. 20220629004).

Cell culture

LX-2 cells were purchased from BeiNa Biological Company (Beijing, China), cultured in Dulbecco's modified Eagle's medium (Gibco, Grand Island, NY, USA), and supplemented with 10% fetal bovine serum. Then, 5 ng/mL TGFβ (ABclonal, Wuhan, China) was used to induce the activation of LX-2. LX-2 cells were treated with 10 mM, 20 mM, 30 mM or 40 mM tanshinone IIA for 24 h. XMU-MP-1 (3 μM) was used as a YAP agonist to treat LX-2 cells for 24 h.

Serum biochemical

Mouse sera were collected, followed by centrifugation and incubation for 30 min at room temperature. The supernatant was collected, and ALT, AST, GSH and MDA levels were directly assessed through Elisa assays, *via* microplate reader. Subsequent experimental procedures were performed according to the manu-

facturer's protocol (C009-3-1, C010-3-1, A006-2-1, A003-1-1; Nanjing Jiancheng Bioengineering Institute, Nanjing, China).

Hematoxylin and eosin (H&E)

Mouse liver samples were collected and fixed with 4% paraformaldehyde at 4°C for 48 h. Then, the samples were dehydrated with an ethanol series, treated with xylene, embedded in paraffin and sectioned into 4 μm thick paraffin sections. The samples were incubated with 0.5% hematoxylin for 5 min and 0.05% eosin for 30 s, followed by dehydration in an ethanol series. Slice images were observed and acquired *via* a light microscope (BX-63; Olympus, Tokyo, Japan) and an accompanying digital camera (DS-Fi3; Nikon, Tokyo, Japan) using a 10× objective.

Sirius red staining

Paraffinized tissue sections were rehydrated and stained with 0.1% Sirius red solution for 1 h. The stained tissues were stained with hematoxylin staining solution for 10 min and dehydrated in 100% ethanol. The samples were mounted and observed under a light microscope (BX-63; Olympus) using a 10× objective.

Immunofluorescence

Paraffin-embedded sections were heated, deparaffinized and rehydrated, then subjected to microwave antigen retrieval in pH 9 EDTA solution for 15 min. After the sections were blocked with 2% BSA for 1 h, primary antibodies against YAP (#14074, 1:200; Cell Signaling Technology, Danvers, MA, USA), α-SMA (ab7817, 1:200; Abbkine Scientific Co., Ltd., Wuhan, China), collagen 1 (66761-1-Ig, 1:200; Proteintech, Wuhan, China), and F4/80 (30325, 1:200; Cell Signaling Technology) were incubated with the sections at 4°C overnight. After washing with TBST three times, the samples were incubated secondary antibodies: goat anti-mouse IgG (H+L), F(ab')2 fragment (4408S, 1:400; Cell Signaling Technology) or goat anti-rabbit IgG (H+L), F (ab')2 fragment (4414S, 1:400; Cell Signaling Technology) diluted with PBS at room temperature for 1 h. For negative controls group, the primary antibody was replaced with 2% BSA. The tissue sections were washed three times with TBST and mounted with DAPI-containing mounting solution, which was prepared by mixing 9 parts glycerol with 1 part PBS and adjusting the pH to 8.5-9.0. A confocal microscope (ECLIPSE Ti A1; Nikon) with 20× and 10× objectives was used for image acquisition. The positive areas were calculated using ImageJ software (National Institutes of Health, Bethesda, MD, USA).

Immunohistochemistry

Most of the steps were the same as those used for immunofluorescence, including the use of 2% BSA for detection in the negative control group. The samples were subjected to hydrogen peroxide treatment for 30 min after microwave antigen retrieval. In addition, the secondary antibodies used for incubation were different: goat anti-rabbit secondary antibodies (8114S, 1:200; Cell Signaling Technology). DAB (cat: 8059; Cell Signaling Technology) was used for color reactions, and a neutral resin sealing sheet was used. Similar to immunofluorescence, image acquisition was performed using a confocal microscope (ECLIPSE Ti A1; Nikon) with 20× and 10× objectives, and ImageJ software was used to quantitatively evaluate the immunolabelling results by measuring the integrated density and area of the positive signals.

RT-PCR

RNA was isolated with TRIzol (Invitrogen, Waltham, MA, USA). Reverse transcription was performed *via* a reverse transcription kit (TaKaRa Bio, Shiga, Japan) containing gDNA erasers. Real-time polymerase chain reaction (PCR) was performed using an ABI 7500 sequence detection system (Applied Biosystems, Foster City, CA, USA) and SYBR Green I (TaKaRa Bio). The data were analyzed *via* a comparative method ($2^{-\Delta\Delta CT}$). The primers used were purchased from Sangon Biotech (Shanghai, China), and their sequences are shown in Table 1.

Western blot

Each cell sample was supplemented with 100 μL of mixed working fluid (RIPA lysate:PMSF = 100:1) and centrifuged at 10000 rpm/min for 10 min. The supernatant was collected, and protein loading buffer was added for denaturation at high temperature. The protein concentration was determined *via* a BCA protein assay system. Protein samples were separated *via* 10-12% SDS-PAGE and transferred to PVDF membranes. The blot was blocked with 5% skim milk in Tris-buffered saline containing 0.1% Tween 20 (TBST) at room temperature for 1 h and then incubated overnight with primary antibodies against α-Tubulin monoclonal (ABL1080, 1:3000; Abbkine Scientific Co., Ltd.), β-actin (ABL1010, 1:3000; Abbkine Scientific Co., Ltd.), Collgen1 (ab316222, 1:1000; Abcam, Cambridge, MA, USA), α-SMA (ET1607-53, 1:5000; HuaBio, Shanghai, China), GPX4 (ET1706-45, 1:10000; HuaBio), YAP (#14074, 1:1000, CST, USA), P-YAP (#13008, 1:1000; Cell Signaling Technology), MOB1 (#13730, 1:1000; Cell Signaling Technology), and MST1 (#3682, 1:1000; Cell Signaling Technology) at 4°C. After washing with TBST three times, the secondary antibodies were conjugated with horseradish peroxidase (goat anti-rabbit, RS23920, ImmunoWay, 1:5000; goat anti-mouse, RS23910, ImmunoWay, 1:5000) and incubated at room temperature for 1 h. Finally, the samples were washed with TBST three times for 5 min each. The specific protein bands were visualized *via* SuperSignal West Pico chemiluminescence substrates and imaged *via* a VersaDoc imaging system (Bio-Rad Laboratories, Hercules, CA, USA).

Iron measurement

Mouse livers (approximately 10 mg) were weighed, lyophilized for 24 h, dissolved in hydrochloric acid and diluted 300 times for measurement *via* Triple Quad-ICP-MS (Agilent, Santa Clara, CA, USA).[25]

Clinical samples

All samples were obtained from the Second Hospital of Lanzhou University, and 26 human liver fibrosis samples were obtained from adjacent liver cancer tissues. Liver fibrosis grades were identified by pathology professionals (S0-1=6, S2-3=10, and S4=10). Informed consent was obtained from all participants, and the study adheres to the principles outlined in the Declaration of Helsinki. The study was approved by the Ethics Committee of the Second Hospital of Lanzhou University (2024A-1237).

Table 1. Primer sequences.

Gene	Primer sequences (5'-3')
α-SMA F	CCCAGACATCAGGGAGTAATGG
α-SMA R	TCTATCGGATACTTCAGCGTCA
COL1A1 F	GCTCCTCTTAGGGGCCACT
COL1A1 R	ATTGGGGACCCTTAGGCCAT
COL3A1 F	CTGTAACATGGAAACTGGGGAAA
COL3A1 R	CCATAGCTGAACTGAAAACCACC
β-actin F	GTGACGTTGACATCCGTAAAGA
β-actin R	GCCGGACTCATCGTACTCC

Bioinformatics analysis

The GSE84044 dataset was obtained from the GEO database and includes 124 liver biopsy samples from CHB patients with different stages of liver fibrosis. All patients were diagnosed according to the Asia-Pacific Association for Liver Studies (APASL) criteria.[26] To study gene dynamics, we sorted the top 2000 genes by absolute median difference (MAD). The K-means algorithm was used to cluster into 4-class gene clusters. Gene Ontology (GO) and Kyoto Encyclopedia of Genes and Genomes (KEGG) analyses and visualization were conducted *via* the "clusterGVis" R package. Additionally, the correlation of YAP1 was calculated *via* Spearman correlation, and we sorted the top 100 genes enriched with the "clusterProfiler" R package. The "ggplot2" R package was used for visualization.

Statistical analysis

Statistical analysis was performed *via* GraphPad Prism 8 (La Jolla, CA, USA). All the data are presented as the means ± SEM. Comparisons were performed by one-way analysis of variance (ANOVA), followed by a Dunnett test. A p-value <0.05 was considered to indicate a significant difference.[26]

Results

Tanshinone IIA alleviated BDL-induced liver fibrosis

H&E staining was used to assess BDL-induced hepatotoxicity. The livers of the sham group of mice had normal lobular structures

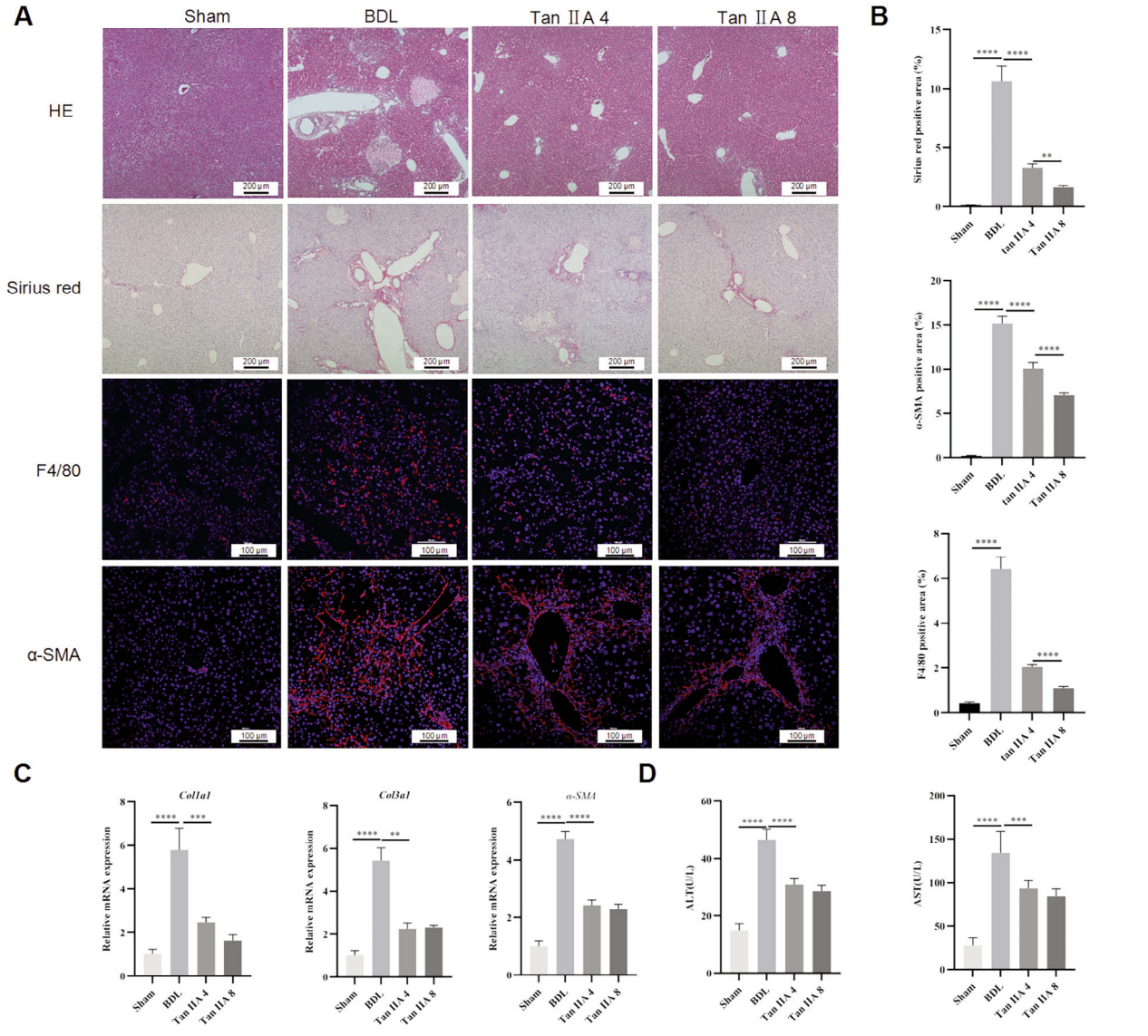

Figure 1. Tanshinone IIA alleviated BDL-induced liver fibrosis and improved liver function. **A**) Pathological features of tanshinone IIA intervention, including H&E and Sirius red staining and F4/80 and α-SMA immunolabelling. **B**) Quantification of Sirius red, F4/80 and α-SMA levels. **C**) *α-SMA, Col1a1* and *Col3a1* mRNA levels. **D**) Serum AST and ALT levels. *p<0.05, *p<0.01, ***p<0.001, ****p<0.0001.

with central veins and radial hepatic cords, whereas those of the BDL group exhibited greater hepatic sinusoid expansion and infiltration of immune cells. Sirius red staining revealed significant collagen deposition in the BDL group compared with the sham group, and pathological features and collagen deposition were reduced in the tanshinone IIA group (Figure 1A-B). In addition, tanshinone IIA inhibited macrophage infiltration (Figure 1A). The *α-SMA, Col1a1* and *Col3a1* mRNA levels were also decreased in the tanshinone IIA group (Figure 1C). The liver function indicators AST and ALT were significantly elevated in the BDL-induced liver fibrosis group and decreased in the tanshinone IIA group (Figure 1D). These findings indicate that tanshinone IIA may ameliorate liver fibrosis and liver function in patients with BDL-induced liver fibrosis.

Tanshinone IIA inhibited HSC activation and collagen production

Tanshinone IIA clearly inhibited the degree of HSC activation relative to that in the BDL group (Figure 1). Considering that HSCs are the main source of collagen production, we treated TGF-β-induced activated LX-2 cells (classic human HSCs) with tanshinone IIA and confirmed that tanshinone IIA can inhibit HSC activation and collagen production in a dose-dependent manner *via* Western blotting and immunofluorescence (Figure 2 A,B).

YAP is upregulated in human liver fibrosis

Considering the importance of YAP in the progression of liver fibrosis, we used a GEO database containing 124 human liver fibrosis samples to analyze the relationship between *YAP* and liver fibrosis. The level of *YAP* increased with fibrosis grade, which was consistent with the expression trends of the liver fibrosis-related genes *CoL1A1, CoL3A1* and *PDGFRB* (Figure 3 A,B). The results of the GO enrichment analysis revealed that these genes are involved in extracellular matrix organization and extracellular structure organization. KEGG analysis revealed that these DEGs were involved mainly in the Hippo signaling pathway, the PI3K-AKT signaling pathway and the TGF-beta signaling pathway (Figure 3C). We further acquired the top 100 genes with positive YAP expression to conduct Gene Ontology (GO) and Kyoto Encyclopedia of Genes and Genomes (KEGG) analyses and GO analyses related to TGF-beta production, cell-surface adhesion and collagen fibril organization. KEGG analysis revealed enriched genes involved in the Hippo signaling pathway and the PI3K-AKT signaling pathway (Figure 3D). These findings indicate that YAP potentially participates in the process of liver fibrosis. To verify this result, we obtained liver fibrosis samples with a definite diagnostic fibrosis grade adjacent to liver cancer and found that YAP expression indeed increased with increasing liver fibrosis grade and that positive expression was found in both hepatocytes and fibrotic areas (Figure 3E).

Tanshinone IIA suppressed YAP signaling and oxidative stress in liver fibrosis

These results indicate that YAP is highly expressed and is positively correlated with fibrosis grade in patients with liver fibrosis. Western blot analysis revealed that tanshinone IIA inhibited the YAP signaling pathway; that of YAP decreased significantly; and that of P-YAP, MST1, and MOB1 increased significantly (Figure 4A). Elevated YAP was observed in BDL-induced liver fibrosis and was widely distributed in the fibrotic area (Figure 4D). In addition, tanshinone IIA also increased the expression of GPX4 and

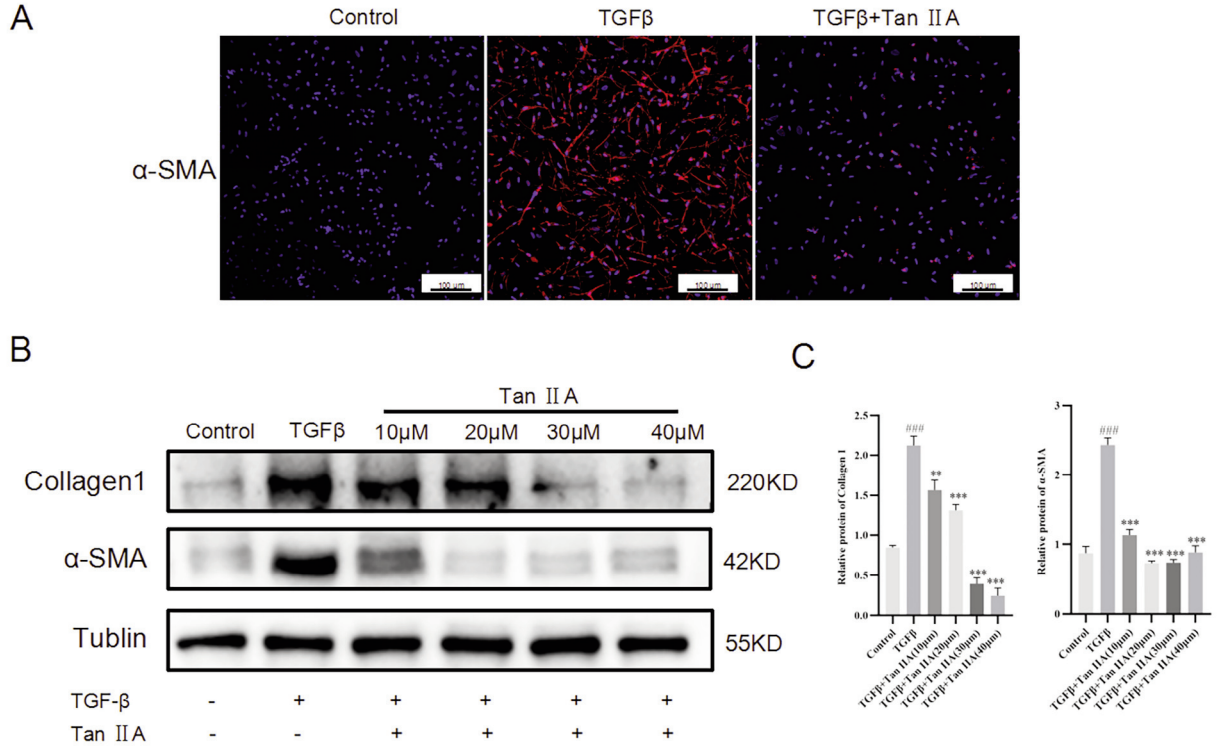

Figure 2. Tanshinone IIA inhibited the activation and collagen 1 production of activated LX-2 cells. Tanshinone IIA (40 mM) inhibited the activation of LX-2, as shown by immunofluorescence (**A**) and Western blotting (**B**). **C**) Statistical plots. **p*<0.05, **p*<0.01, ****p*<0.001, *****p*<0.0001 (tanshinone IIA group *vs* TGFβ group); #*p*<0.05, ##*p*<0.01, ###*p*<0.001, ####*p*<0.001 (TGFβ group *vs* control).

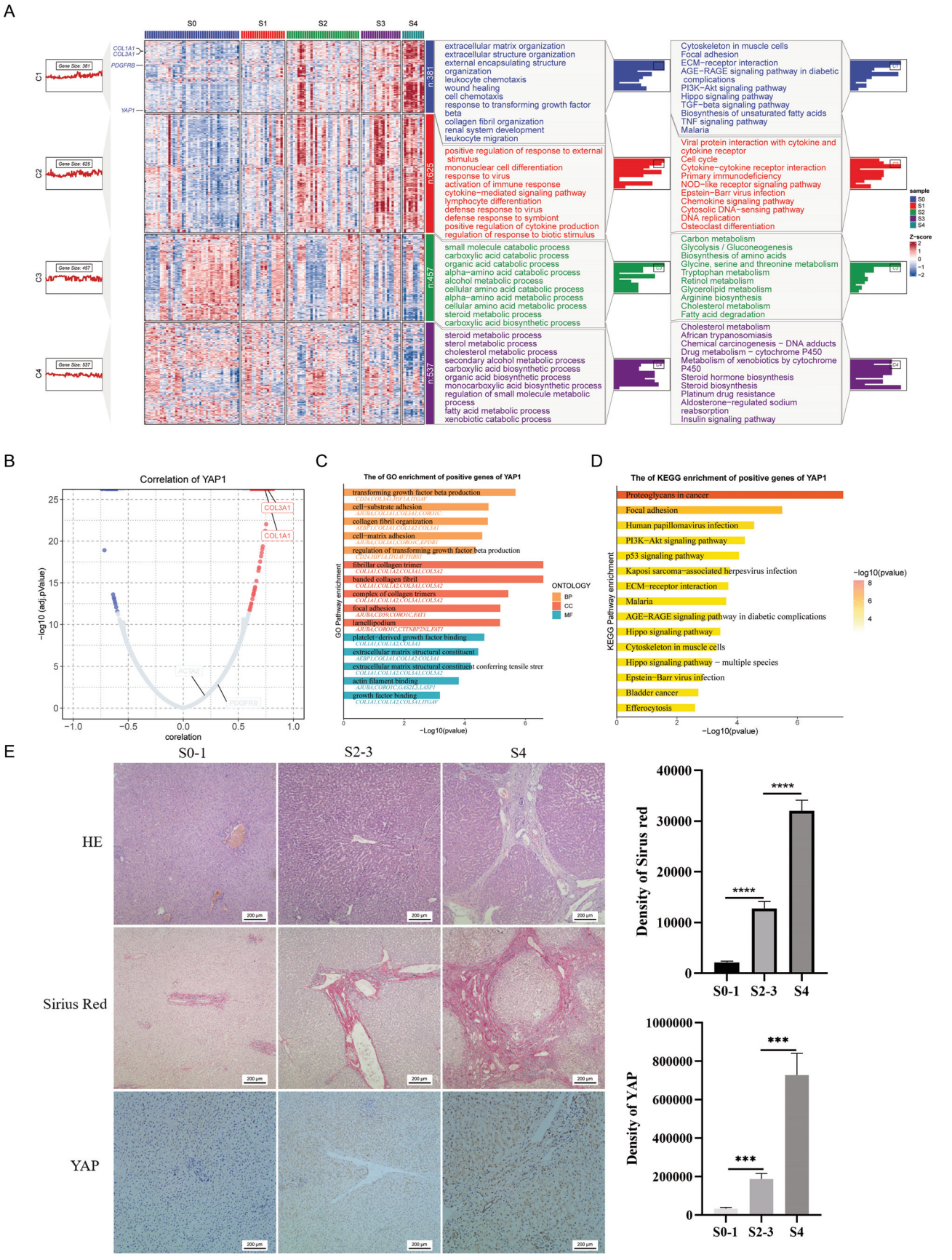

Figure 3. YAP involvement in the progression of liver fibrosis according to bioinformatics analysis and human samples. **A**) Heatmap, GO and KEGG analyses of DEGs. **B**) Genes positive for YAP. **C,D**) GO and KEGG analyses of the positively correlated genes. **E**) YAP expression increased with increasing fibrosis grade in human livers; statistical plots are shown on the right. *p<0.05, **p<0.01, ***p<0.001.

GSH (Figure 4 A,C,E), and the total iron and MDA levels were reduced (Figure 4C). This evidence suggests that tanshinone IIA inhibits YAP signaling pathway oxidative stress and liver fibrosis.

Tanshinone IIA inhibited YAP signaling in activated HSCs

TGFβ-treated HSCs can be activated and express high α-SMA levels. We observed that activated HSCs significantly increased YAP expression. Like in BDL-induced liver fibrosis, tanshinone IIA inhibited YAP expression and TGFβ-induced HSC activation (Figure 5A). Western blot analysis also revealed that HSC activation is accompanied by the upregulation of YAP signaling, and tanshinone IIA inhibited HSC activation and YAP signaling (Figure 5B). In addition, tanshinone IIA decreased GPX4 expression in activated HSCs, potentially promoting ferroptosis in activated HSCs. This evidence suggests that tanshinone IIA may inhibit HSC activation and promote HSC ferroptosis by inhibiting YAP signaling.

Tanshinone IIA inhibited the activation of HSCs by suppressing YAP signaling

To further clarify whether tanshinone IIA exerts antifibrotic

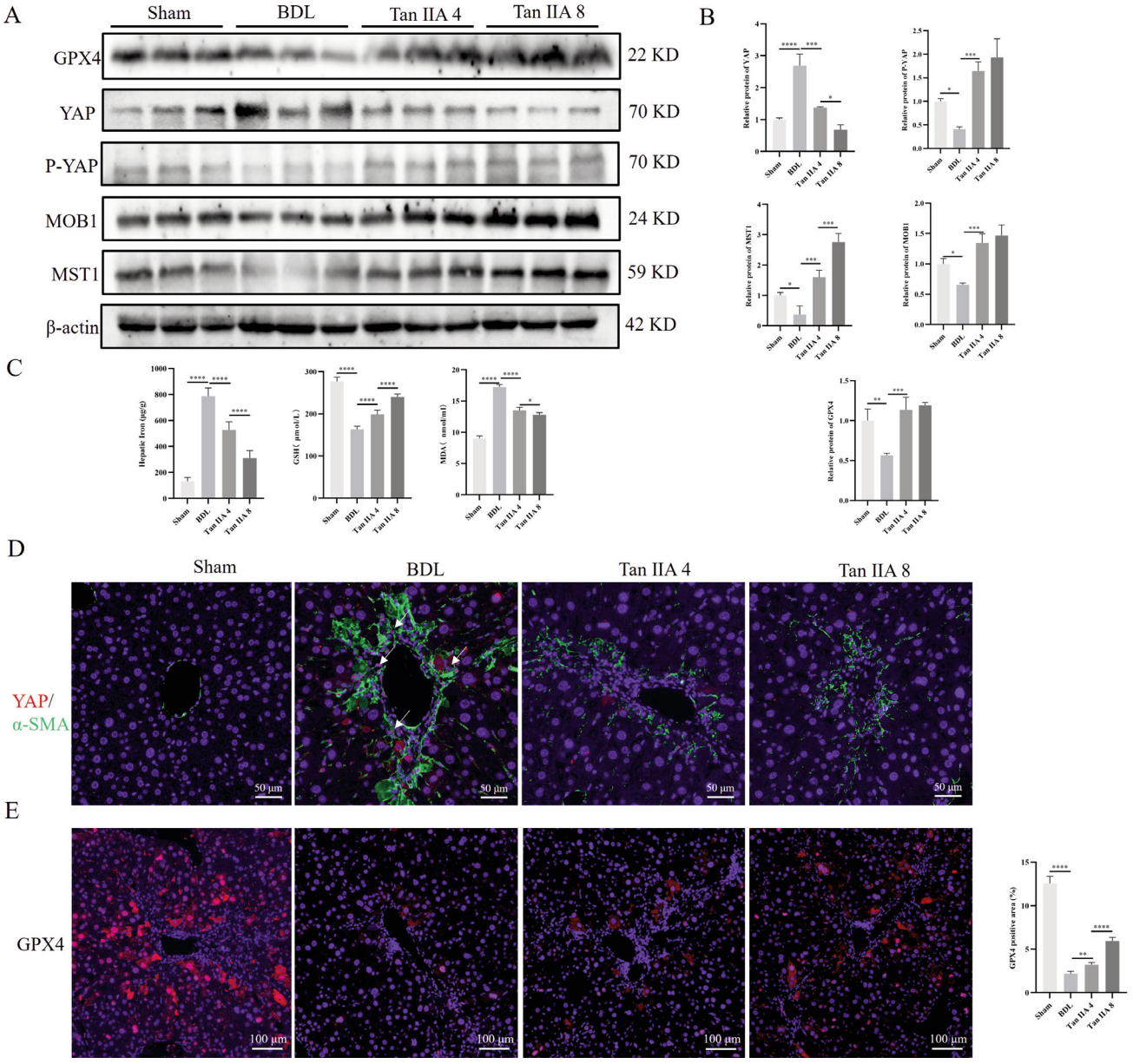

Figure 4. Tanshinone IIA inhibited YAP signaling, oxidative stress, and liver fibrosis. **A**) Western blot analysis revealed that tanshinone IIA inhibited the expression of YAP and promoted the expression of P-YAP and GPX4 in BDL-induced liver fibrosis. **B**) Statistical plots of the WB data are shown on the corresponding right side. **C**) Tanshinone IIA reduced iron accumulation and MDA and increased the GSH level in liver fibrosis. **D**) Immunofluorescence revealed that tanshinone IIA inhibited the expression of YAP and α-SMA and the nuclear translocation of YAP in HSCs in the BDL model. **E**) Immunofluorescence revealed that tanshinone IIA promoted the expression of GPX4 in the BDL model. *p<0.05, *p<0.01, ***p<0.001, ****p<0.0001 (tanshinone IIA group *vs* BDL group); $^{\#}p$<0.05, $^{\#\#}p$<0.01, $^{\#\#\#}p$<0.001, $^{\#\#\#\#}p$<0.001. (BDL group *vs* control).

effects through YAP signaling, we combined the YAP agonist XMU-MP-1 (XM1) with tanshinone IIA to treat TGFβ-treated HSCs. XM1 significantly reversed tanshinone IIA-induced decreases in YAP expression, HSC inactivation and collagen production (Figure 6 A-C). In addition, XM1 also elevated GPX4 expression. The above results showed that tanshinone IIA inhibited HSC activation by suppressing YAP signaling.

The YAP agonist XMU reversed the effect of tanshinone IIA on liver fibrosis

Finally, to further explore whether tanshinone IIA exerts a therapeutic effect on liver fibrosis through YAP, we performed an *in vivo* experiment in which tanshinone IIA was combined with the YAP agonist XM1. We observed that XMU significantly reversed the therapeutic effect of tanshinone IIA on liver fibrosis, increased the number of activated HSCs and infiltrating macrophages and aggravated pathological features (Figure 7). In addition, XMU inhibited the effects of tanshinone on the iron load and MDA content and increased the GSH and GPX4 levels. Overall, YAP is a key regulator in the process of tanshinone IIA treatment of liver fibrosis.

Discussion

Liver fibrosis is an intermediate pathological process of all end-stage liver diseases that is reversible, and the treatment of liver fibrosis can greatly alleviate the occurrence and progression of

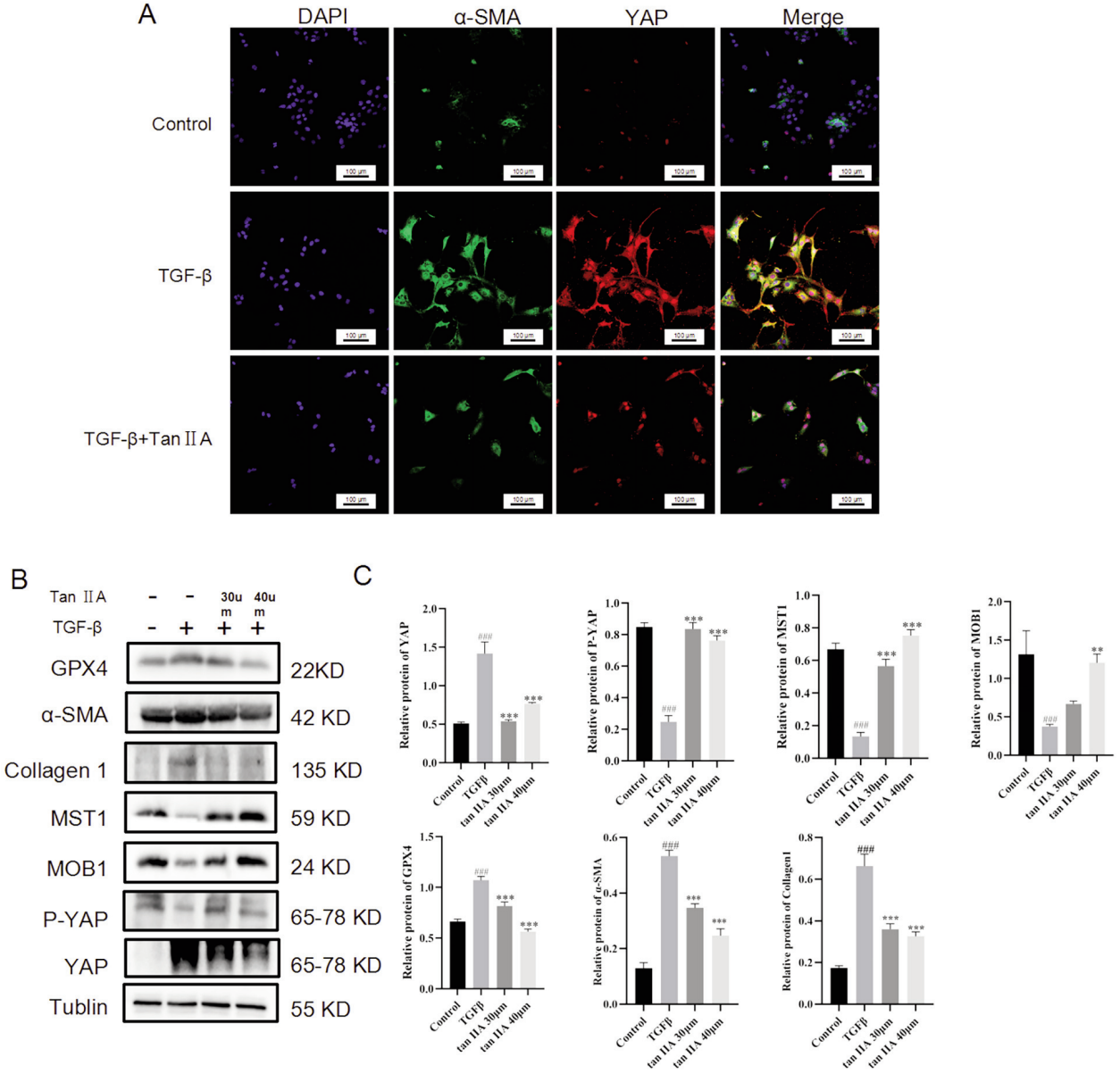

Figure 5. Tanshinone IIA inhibited TGF-β-induced LX-2 activation, collagen 1 production, and the YAP signaling pathway. **A**) Immunofluorescence revealed that tanshinone IIA inhibited α-SMA expression and that the expression of YAP induced by TGF-β activated LX-2 cells. **B**) Western blot analysis revealed that tanshinone IIA inhibited α-SMA and collagen 1 expression and that YAP signaling induced by TGF-β activated LX-2 cells. **C**) Statistical plots of the Western blot data. *p<0.05, **p<0.01, ***p<0.001, ****p<0.0001.

malignant liver disease. The prevention and treatment of liver fibrosis has important clinical significance.[27,28] Traditional Chinese medicine has the advantages of multiple targets and low cost, so it has great potential in the treatment of liver fibrosis. In this study, tanshinone IIA, which has antioxidant stress and anti-inflammatory functions, was investigated to explore whether it has anti-liver fibrosis effects and its potential pathogenesis. The results showed that tanshinone IIA inhibited the inflammatory response and HSC activation and alleviated oxidative stress and BDL-induced liver fibrosis through the Hippo–YAP signaling pathway.

Given the limited studies on the anti-liver fibrosis effects of tanshinone II A, we first established classic BDL models to further clarify whether tanshinone II A has therapeutic effects on liver fibrosis. Pathological findings revealed that tanshinone II A significantly reduced inflammatory cell infiltration, collagen deposition, HSC activation and the progression of liver fibrosis.

Similarly, we also verified the antifibrotic effect of tanshinone II A *via* cell experiments. Tanshinone IIA clearly inhibited the HSC activation and collagen production induced by TGFβ. Next, we explored the anti-liver fibrosis mechanism of tanshinone IIA. Many clinical studies have shown that patients with liver fibrosis often experience severe YAP overload.[29,30] YAP expression increases during the development of liver fibrosis and decreases during the reversal of liver fibrosis.[12,30-33] Silencing of YAP contributes to the reversal of liver fibrosis and may be a valid target for activation of HSCs.[33-35] Therefore, targeting YAP is an effective strategy for the prevention and treatment of liver fibrosis. In our *in vitro* and *in vivo* experiments, an increase in the YAP level was confirmed in a fibrosis model, and YAP was expressed in the nucleus of HSCs. These findings indicate that activated HSCs are in an active state of proliferation. Tanshinone IIA suppressed YAP upregulation, HSC activation and collagen formation. Therefore, tanshinone IIA can inhibit YAP signaling and liver fibrosis.

To clarify the role of YAP in alleviating liver fibrosis, tanshinone IIA was used. We applied the YAP agonist XMU-MP-1 (XMU) combined with tanshinone IIA to treat LX-2 activated by TGFβ.[36,37] XMU, an MST1/2 kinase inhibitor located upstream of YAP and negatively regulating YAP *via* LAST1/2 phosphorylation,

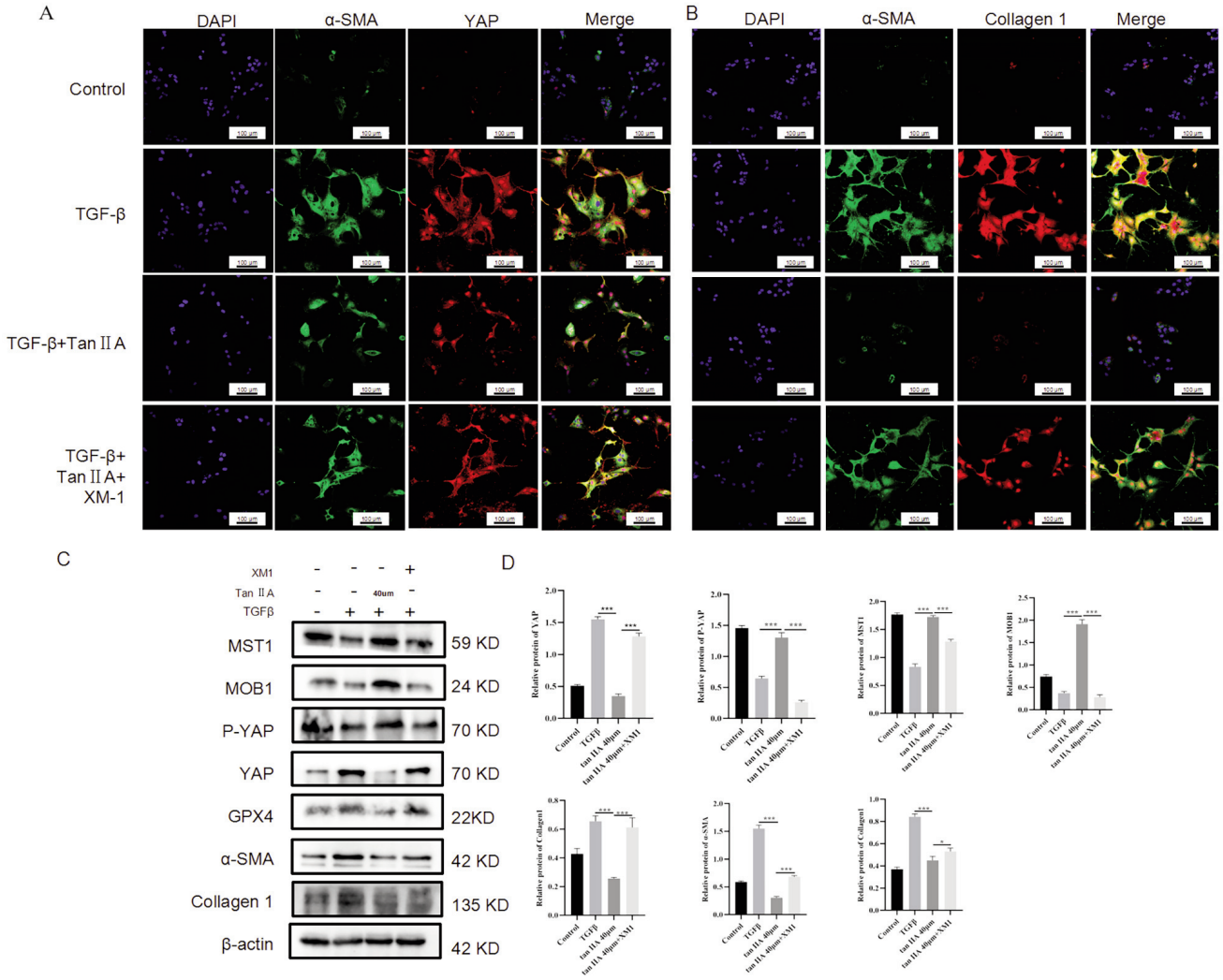

Figure 6. Tanshinone IIA inhibited the activation of LX-2 via the inhibition of the YAP signaling pathway. **A,B**) Immunofluorescence showed that tanshinone IIA inhibited LX-2 activation and collagen production by inhibiting YAP. **C,D**) Western blot analysis revealed that tanshinone IIA suppressed LX-2 activation by inhibiting YAP. *p<0.05, **p<0.01, ***p<0.001, ****p<0.0001.

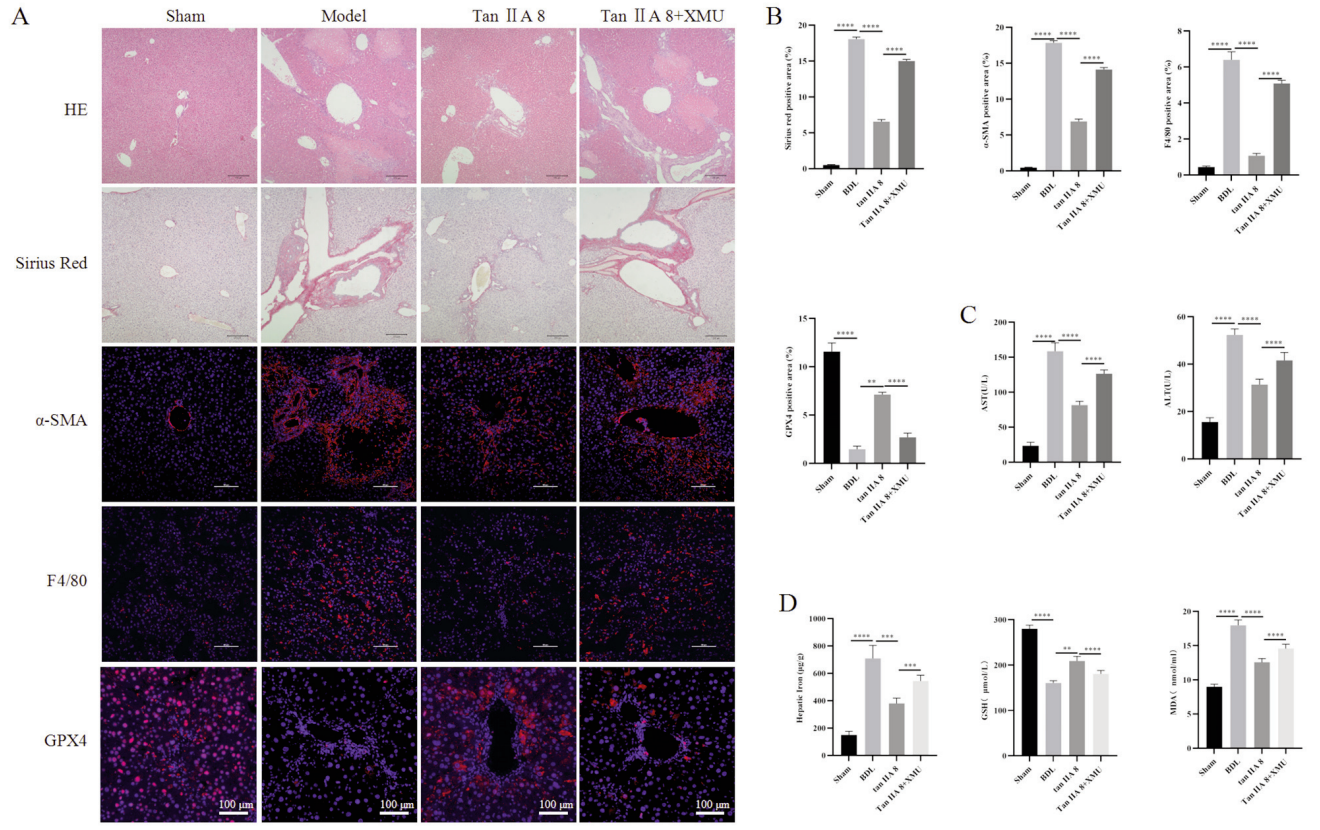

Figure 7. The YAP inhibitor XMU reversed the therapeutic effect of tanshinone IIA on liver fibrosis. **A**) Pathological effects of the YAP inhibitor XMU on the therapeutic effects of tanshinone IIA, including H&E, Sirius red, F4/80, α-SMA, and GPX4. **B**) Quantification of Sirius red, F4/80, α-SMA and GPX4 expression. **C**) Serum AST and ALT levels. **D**) Changes in iron content and MDA and GSH levels. *p<0.05, **p<0.01, ***p<0.001, ****p<0.0001.

is widely used as a YAP agonist.[38,39] XMU reversed the inhibitory effects of tanshinone IIA on activated HSCs. Considering the limitations of the *in vitro* experiments, we treated the BDL model together with tanshinone IIA and XMU and found that the therapeutic effect of tanshinone IIA was also reversed. The above results demonstrated that tanshinone IIA can exert its anti-liver fibrosis effect by blocking YAP signaling.

Interestingly, we found that tanshinone IIA can decrease iron and MDA levels and increase GPX4 and GSH in liver fibrosis. These compounds are all indicators related to oxidative stress, suggesting that tanshinone IIA can significantly inhibit oxidative stress in the liver. However, the YAP agonist XMU reversed the treatment process. Therefore, tanshinone IIA-mediated YAP signaling has antioxidant and anti-inflammatory effects, inhibits HSC activation and alleviates liver fibrosis.

In conclusion, our data preliminarily confirmed that tanshinone IIA improved BDL-induced liver fibrosis progression and HSC activation *via* YAP. Owing to the limited funds, the mechanism exploration was also rather superficial, and the model observation time was not long enough, which all deserve further investigation in the future.

References

1. Hammerich L, Tacke F. Hepatic inflammatory responses in liver fibrosis. Nat Rev Gastroenterol Hepatol 2023;20:633-46.
2. Henderson NC, Rieder F, Wynn TA. Fibrosis: from mechanisms to medicines. Nature 2020;587:555-66.
3. Huang DQ, Terrault NA, Tacke F, Gluud LL, Arrese M, Bugianesi E, et al. Global epidemiology of cirrhosis - aetiology, trends and predictions. Nat Rev Gastroenterol Hepatol 2023;20:388-98.
4. Moroni F, Dwyer BJ, Graham C, Pass C, Bailey L, Ritchie L, et al. Safety profile of autologous macrophage therapy for liver cirrhosis. Nat Med 2019;25:1560-5.
5. GBD 2017 Cirrhosis Collaborators. The global, regional, and national burden of cirrhosis by cause in 195 countries and territories, 1990-2017: a systematic analysis for the Global Burden of Disease Study 2017. Lancet Gastroenterol Hepatol 2020;5:245-66.
6. Jepsen P, Younossi ZM. The global burden of cirrhosis: A review of disability-adjusted life-years lost and unmet needs. J Hepatol 2021;75 Suppl 1:S3-s13.
7. Schuppan D, Kim YO. Evolving therapies for liver fibrosis. J Clin Invest 2013;123:1887-901.
8. Zhang CY, Yuan WG, He P, Lei JH, Wang CX. Liver fibrosis and hepatic stellate cells: Etiology, pathological hallmarks and therapeutic targets. World J Gastroenterol 2016;22:10512-22.
9. Cai X, Wang J, Wang J, Zhou Q, Yang B, He Q, et al. Intercellular crosstalk of hepatic stellate cells in liver fibrosis: New insights into therapy. Pharmacol Res 2020;155:104720.
10. Du K, Maeso-Díaz R, Oh SH, Wang E, Chen T, Pan C, et al. Targeting YAP-mediated HSC death susceptibility and senescence for treatment of liver fibrosis. Hepatology 2023;77:1998-2015.

11. Tong G, Chen X, Lee J, Fan J, Li S, Zhu K, et al. Fibroblast growth factor 18 attenuates liver fibrosis and HSCs activation via the SMO-LATS1-YAP pathway. Pharmacol Res 2022;178:106139.
12. Lu ZN, Niu WX, Zhang N, Ge MX, Bao YY, Ren Y, et al. Pantoprazole ameliorates liver fibrosis and suppresses hepatic stellate cell activation in bile duct ligation rats by promoting YAP degradation. Acta Pharmacol Sin 2021;42:1808-20.
13. Philippe MA, Ruddell RG, Ramm GA. Role of iron in hepatic fibrosis: one piece in the puzzle. World J Gastroenterol 2007;13:4746-54.
14. Zhao W, Lei M, Li J, Zhang H, Zhang H, Han Y et al. Yes-associated protein inhibition ameliorates liver fibrosis and acute and chronic liver failure by decreasing ferroptosis and necroptosis. Heliyon 2023;9:e15075.
15. Chen L, Jin X, Ma J, Xiang B, Li X. YAP at the progression of inflammation. Front Cell Dev Biol 2023;11:1204033.
16. Jiang Z, Gao W, Huang L. Tanshinones, critical pharmacological components in Salvia miltiorrhiza. Front Pharmacol 2019;10:202.
17. Yang L, Wang Y, Wang X, Liu Y. Effect of allogeneic umbilical cord mesenchymal stem cell transplantation in a rat model of hepatic cirrhosis. J Tradit Chin Med 2015;35:63-8.
18. Chen Z, Xu H. Anti-Inflammatory and Immunomodulatory mechanism of tanshinone iia for atherosclerosis. Evid Based Complement Alternat Med 2014;2014:267976.
19. Meng Z, Meng L, Wang K, Li J, Cao X, Wu J et al. Enhanced hepatic targeting, biodistribution and antifibrotic efficacy of tanshinone IIA loaded globin nanoparticles. Eur J Pharm Sci 2015;73:35-43.
20. Bi Z, Wang Y, Zhang W. A comprehensive review of tanshinone IIA and its derivatives in fibrosis treatment. Biomed Pharmacother 2021;137:111404.
21. Ying Q, Teng Y, Zhang J, Cai Z, Xue Z. Therapeutic effect of tanshinone IIA on Liver fibrosis and the possible mechanism: a preclinical meta-analysis. Evid Based Complement Alternat Med 2019;2019:7514046.
22. Li H, Hu P, Zou Y, Yuan L, Xu Y, Zhang X, et al. Tanshinone IIA and hepatocellular carcinoma: A potential therapeutic drug. Front Oncol 2023;13:1071415.
23. Li Q, Huang D, Liao W, Su X, Li J, Zhang J, et al. Tanshinone IIA regulates CCl(4) induced liver fibrosis in C57BL/6J mice via the PI3K/Akt and Nrf2/HO-1 signaling pathways. J Biochem Mol Toxicol 2024;38:e23648.
24. Yang N, Chen H, Gao Y, Zhang S, Lin Q, Ji X, et al. Tanshinone IIA exerts therapeutic effects by acting on endogenous stem cells in rats with liver cirrhosis. Biomed Pharmacother 2020;132:110815.
25. Wei M, Huang Q, Dai Y, Zhou H, Cui Y, Song W, et al. Manganese, iron, copper, and selenium co-exposure and osteoporosis risk in Chinese adults. J Trace Elem Med Biol 2022;72:126989.
26. Wang M, Gong Q, Zhang J, Chen L, Zhang Z, Lu L, et al. Characterization of gene expression profiles in HBV-related liver fibrosis patients and identification of ITGBL1 as a key regulator of fibrogenesis. Sci Rep 2017;7:43446.
27. Affo S, Yu LX, Schwabe RF. The role of cancer-associated fibroblasts and fibrosis in liver cancer. Annu Rev Pathol 2017;12:153-86.
28. Bardou-Jacquet E, Morandeau E, Anderson GJ, Ramm GA, Ramm LE, Morcet J, et al. Regression of fibrosis stage with treatment reduces long-term risk of liver cancer in patients with hemochromatosis caused by mutation in HFE. Clin Gastroenterol Hepatol 2020;18:1851-7.
29. Zhubanchaliyev A, Temirbekuly A, Kongrtay K, Wanshura LC, Kunz J. Targeting Mechanotransduction at the transcriptional level: YAP and BRD4 Are novel therapeutic targets for the reversal of liver fibrosis. Front Pharmacol 2016;7:462.
30. Xu L, Wettschureck N, Bai Y, Yuan Z, Wang S. Myofibroblast YAP/TAZ is dispensable for liver fibrosis in mice. J Hepatol 2021;75:238-41.
31. Shan S, Liu Z, Liu Z, Zhang C, Song F. MitoQ alleviates carbon tetrachloride-induced liver fibrosis in mice through regulating JNK/YAP pathway. Toxicol Res (Camb) 2022;11:852-62.
32. Martin K, Pritchett J, Llewellyn J, Mullan AF, Athwal VS, Dobie R, et al. PAK proteins and YAP-1 signalling downstream of integrin beta-1 in myofibroblasts promote liver fibrosis. Nat Commun 2016;7:12502.
33. Yang T, Wu E, Zhu X, Leng Y, Ye S, Dong R ,et al. TKF, a mexicanolide-type limonoid derivative, suppressed hepatic stellate cells activation and liver fibrosis through inhibition of the YAP/Notch3 pathway. Phytomedicine 2022;107:154466.
34. Kim CW, Yoon Y, Kim MY, Baik SK, Ryu H, Park IH, et al. 12-O-tetradecanoylphorbol-13-acetate reduces activation of hepatic stellate cells by inhibiting the hippo pathway transcriptional coactivator YAP. Cells 2022;12:91.
35. Bruschi FV, Tardelli M, Einwallner E, Claudel T, Trauner M. PNPLA3 I148M up-regulates hedgehog and yap signaling in human hepatic stellate cells. Int J Mol Sci 2020;21:8711.
36. Barrette AM, Ronk H, Joshi T, Mussa Z, Mehrotra M, Bouras A, et al. Anti-invasive efficacy and survival benefit of the YAP-TEAD inhibitor verteporfin in preclinical glioblastoma models. Neuro Oncol 2022;24:694-707.
37. Tsai HC, Tsai MH, Hua CH, Huang CW, Lu CC, Chen KJ, et al. Circ_0002722-induced regulation of YAP promotes platinum resistance in oral squamous cell carcinoma: Implications for verteporfin therapy. Biochem Pharmacol 2024;229:116460.
38. Sahu MR, Ahmad MH, Mondal AC. MST1 selective inhibitor Xmu-mp-1 ameliorates neuropathological changes in a rat model of sporadic Alzheimer's disease by modulating hippo-Wnt signaling crosstalk. Apoptosis 2024;29:1824-1851.
39. Zhou X, Wang H, Li D, Song N, Yang F, Xu W. MST1/2 inhibitor XMU-MP-1 alleviates the injury induced by ionizing radiation in haematopoietic and intestinal system. J Cell Mol Med 2022;26:1621-8.

Received: 1 April 2025. Accepted: 6 May 2025.

European Journal of Histochemistry 2025; 69:4218
doi:10.4081/ejh.2025.4218